

Laser photoelectron spectroscopy of CrH^- , CoH^- , and NiH^- : Periodic trends in the electronic structure of the transition-metal hydrides

Amy E. Stevens Miller,^{a)} C. S. Feigerle,^{b)} and W. C. Lineberger

Department of Chemistry and Biochemistry, University of Colorado, and Joint Institute for Laboratory Astrophysics, University of Colorado and National Bureau of Standards, Boulder, Colorado 80309-0440

(Received 26 January 1987; accepted 16 April 1987)

The laser photoelectron spectra of CrH^- , CoH^- , and NiH^- and the analogous deuterides are reported. The spectra are interpreted using a qualitative description of the electronic structure for the hydrides. This model is used to assign off-diagonal transitions in the photodetachment to low-spin states of the neutrals, and diagonal transitions to high-spin states of the neutrals. These data are used to identify the high-spin states of CoH and NiH ; several other states of CrH , CoH , and NiH are also identified. Periodic trends in the bond lengths, vibrational frequencies, and electronic excitation energies for the MnH through NiH molecules are examined. Electron affinities are reported for CrH (0.563 ± 0.010 eV), CoH (0.671 ± 0.010 eV), and NiH (0.481 ± 0.007 eV), and the corresponding deuterides.

I. INTRODUCTION

We recently reported the photoelectron spectra of MnH^- and FeH^- ,¹ and interpreted these spectra using a qualitative model for the electronic structure of the diatomic transition-metal hydrides of the latter half of the periodic table.² In this model, bonding of the metal and hydrogen atoms occurs through the s electrons and the d electrons remain largely core, nonbonding electrons. The simplest application of this model yields two types of metal-hydrogen bonding. States of $d^k s^2$ configuration of the metal atom will bond to the incoming hydrogen by forming a $d^k \sigma^2 \sigma^{*1}$ high-spin configuration in the metal-hydride (MH) molecule, where one of the metal $4s$ electrons forms the sigma bond to the hydrogen, and the other becomes a σ^* electron, somewhat antibonding with respect to the M-H bond. Alternatively, bonding to states of $d^{k+1} s^1$ configuration of the metal atom will result in the low-spin, $d^{k+1} \sigma^2$ configuration for MH . Schematic potential energy curves for states of these two configurations are shown in Fig. 1. The high-spin states of the MH , because of the antibonding nature of the σ^* electron, will have a longer bond length and lower vibrational frequency than the low-spin states. This difference in bond lengths for the two states together with arguments for the MX^- ground state configuration are the key elements in the interpretation of the negative-ion photoelectron spectra.

Based largely on the overwhelming stability³ of the $d^{k+1} s^2$ configuration (as compared to the $d^{k+2} s^1$ configuration) for M^- , the lowest energy state of MH^- is predicted to have the high-spin configuration $d^{k+1} \sigma^2 \sigma^{*1}$. With this configuration for MH^- , photodetachment to both low-spin and high-spin states of the neutral are one-electron allowed, but the transitions can be distinguished by the vibrational signatures of the photoelectron spectrum. Loss of the anti-

bonding electron from MH^- will result in a large geometry change in a transition to the low-spin state of the neutral MH , and a spectroscopic signature of a long vibrational progression in this off-diagonal transition. Conversely, detachment of the d , nonbonding core electron from MH^- will result in a high-spin MH with bond length comparable to MH^- and a resulting diagonal transition with a very limited vibrational progression in the photoelectron spectrum. Indeed, this model was successfully employed to interpret the photoelectron spectrum of MnH^- as due to transitions to the known⁴⁻⁷ high-spin ground state, $^7\Sigma^+$, and an excited low-spin state of MnH . The low-spin excited state has not been observed spectroscopically, nor have calculations been reported for this state.

This model was also applied to the FeH^- spectrum to give a low-spin, $^4\Delta$ ground state, with an excited high-spin, $^6\Delta$ state quite close in energy for FeH . Since this report, the unassigned FeH infrared transition at about 9965 cm^{-1} (which we had proposed as a ground state $^4\Delta$ to an excited quartet state transition) has now been analyzed as a $^4\Delta-^4\Delta$ transition.^{8,9} Calculations on the $^4\Delta$ and $^6\Delta$ states of FeH have been reported by Walch and Bauschlicher,¹⁰ Walch,¹¹ Krauss and Stevens,¹² Chong *et al.*,¹³ and Dolg *et al.*¹⁴ Walch¹¹ and Dolg *et al.*¹⁴ also reported calculations on the $^5\Delta$ state of FeH^- . Although these authors emphasize the extensive configuration interaction in the electronic structure of these molecules, including strong ionic contributions to the $^6\Delta$ state of FeH and the $^5\Delta$ state of FeH^- , all their calculations provide excellent corroboration of our assignment of a low-spin ground state for FeH . Thermochemical data also support this assignment. Squires¹⁵ interprets the weak Fe-H bond energy, 29.6 ± 3 kcal/mol,¹⁶ as being due to the high promotion energy of the Fe atom to the $3d^7 4s^1$ bonding configuration, consistent with our assignment. Recent spectroscopic studies of matrix-isolated¹⁷ and gas-phase MnH ¹⁸ suggest somewhat more complex bonding than our model.

We report here photoelectron spectra of CrH^- , CoH^- , and NiH^- , and the analogous deuterides for each molecule. The photoelectron spectra of these ions are analyzed using

^{a)} Present address: Department of Chemistry, University of Oklahoma, Norman, Oklahoma 73019.

^{b)} Present address: Department of Chemistry, University of Tennessee, Knoxville, Tennessee 37996.

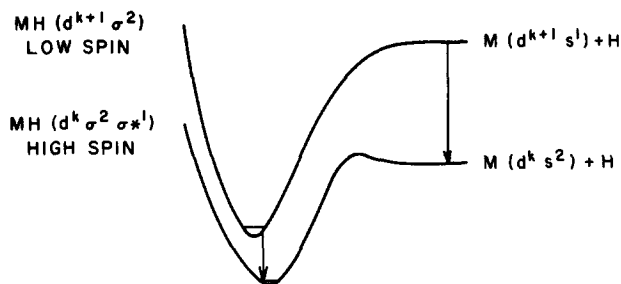


FIG. 1. Illustration of the bonding potential curves for the high-spin and low-spin states of the metal hydrides. Arrows indicate the energy differences in the atomic states, $E(d^{k+1} s^1) - E(d^k s^2)$, and the molecular states $E(d^{k+1} \sigma^2) - E(d^k \sigma^2 \sigma^{*1})$. The dependence of the energy separation of the molecular states on the atomic state energy is discussed in the text and illustrated in Fig. 5.

this simple s electron bonding model and are consistent with other spectroscopic studies which have identified the ground states of CrH ,¹⁹⁻²¹ CoH ,^{22,23} and NiH ²³⁻²⁷ to be ${}^6\Sigma^+$, ${}^3\Phi$, and ${}^2\Delta$, respectively. Electron affinities (EA) are obtained for each of the molecules involved, and several previously unidentified excited states of the molecules are observed. Periodic trends in the bond lengths, vibrational frequencies, and electronic excitation energies are provided from these and other optical spectroscopic data.

II. EXPERIMENTAL

The experimental apparatus²⁸ for negative ion photoelectron spectroscopy begins with an electrical discharge ion source, from which negative ions are extracted, accelerated to 680 eV, and mass analyzed by a Wien filter. The mass-analyzed beam is crossed with the photons of a cw argon-ion laser operating intracavity; the 488.0 nm (2.540 eV) line, which provides about 100 W circulating power, is used for photodetachment. Photodetached electrons ejected perpendicular to the laser and ion beams are energy analyzed in a hemispherical energy analyzer, with resolution approximately 45 meV FWHM. The data for CoH^- and CoD^- were obtained using a newer version of the analyzer, described elsewhere,²⁹ with resolution approximately 12 meV FWHM. The absolute, center-of-mass electron kinetic energies are determined as described elsewhere for the two analyzers.^{1,29}

CrH^- , CoH^- , NiH^- , and the corresponding deuterides were produced from a mixture of the appropriate metal carbonyl [$\text{Cr}(\text{CO})_6$, $\text{Co}(\text{CO})_3\text{NO}$, $\text{Ni}(\text{CO})_4$] and NH_3 (ND_3) in the discharge source. These mixtures produced not only MH^- but M^- and MH_2^- as well. Limited mass resolution and the presence of multiple metal isotopes did not allow a pure MH^- beam to be isolated. This frequently necessitated subtraction of the spectra^{3,30,31} of M^- or MH_2^- (MD_2^-) from the spectrum of MH^- (MD^-). In most cases, photoelectron peaks from the different species were well separated in the spectrum and a clean subtraction was obtained; in instances where some overlap of peaks occurs, the effect on the spectrum is noted in the figures and the text. All spectra were fitted and analyzed using the Franck-Condon factor procedure developed for MnH^- and FeH^- and discussed in detail elsewhere.¹

III. RESULTS

A. Spectra of CoH^- and CoD^-

The photoelectron spectra of CoH^- and CoD^- , obtained with 2.54 eV photons are shown in Fig. 2. Two peaks, labeled X and A in each of the spectra, occur at essentially the same electron kinetic energy in both the CoH^- and CoD^- spectra, and are thus assigned as (0,0) transitions. A vibrational progression is built off of peak X in both spectra. The CoH (CoD) vibrational frequency is determined to be $1835 \pm 40 \text{ cm}^{-1}$ ($1325 \pm 40 \text{ cm}^{-1}$) from the corresponding spectra, in excellent agreement with reported gas-phase values.²² The assignment of these spectra is quite straightforward, since the CoH ground state is known to be a ${}^3\Phi$ state with low-spin configuration $d^8 \sigma^2$. The ground state of the negative ion is expected to be the high-spin, $d^8 \sigma^2 \sigma^{*1}$ configuration, with ${}^4\Phi$ symmetry. The observation of the vibrational progression in the transition from CoH^- to the ground state CoH is thus completely consistent with the loss of the somewhat antibonding σ^* electron and a relatively large geometry change in detachment to the low-spin state.

The transition to peak A is diagonal, with only a (0,0) peak evident. The lack of a vibrational progression in the detachment to peak A indicates it is the result of a transition in which a d , nonbonding electron is ejected in detachment to a high-spin CoH , with configuration $d^7 \sigma^2 \sigma^{*1}$. Possible candidates for the CoH ($d^7 \sigma^2 \sigma^{*1}$) final state in this transi-

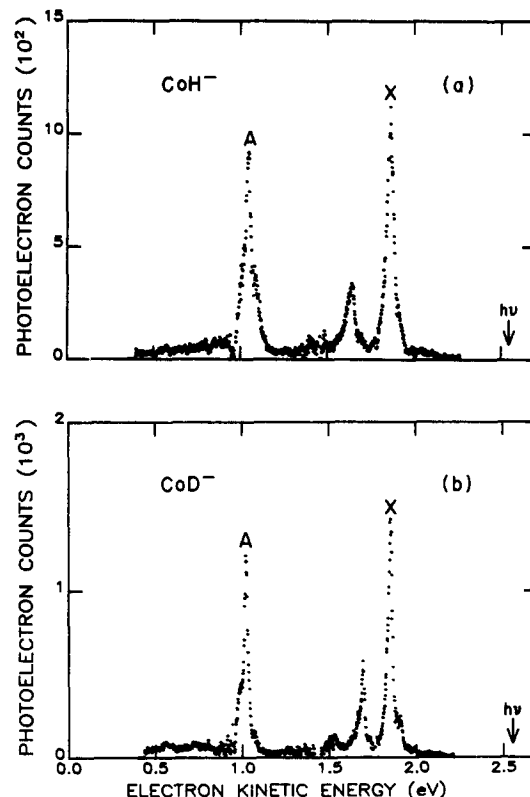


FIG. 2. Photoelectron spectra of CoH^- and CoD^- obtained with 488.0 nm (2.540 eV) photons. The (0,0) transitions result in peaks X and A in the spectra. Scatter in the data points at about 0.9 eV and 1.4 eV are the result of statistical errors in the subtraction of the spectra of CoH_2^- (or CoD_2^-) and Co^- .

TABLE I. Spectroscopic constants for the states of CoH and CoH⁻ observed in the photoelectron spectra. The data for CoD⁻ and CoD are given in parentheses, below the constants reported for the hydride.

Predominant electron configuration and state assignment	EA (eV)	T_0 (cm ⁻¹)	ω_e (cm ⁻¹)	$\omega_e x_e$ (cm ⁻¹)	ν_{01} (cm ⁻¹)	r_e (Å)
CoH						
$a d^7 \sigma^2 \sigma^{*1} (^5\Phi)^a$		6625 ± 110 (6756 ± 110)		1.67 ± 0.05 (1.63 ± 0.05)
$X d^8 \sigma^2 {}^3\Phi$	0.671 ± 0.010 (0.680 ± 0.010)	0 (0)	1925.2 ^b (1373.22) ^c	34.6 ^b (17.59) ^c	1856 ^b (1338.04) ^c	1.542 ^b (1.5179) ^c
CoH ⁻						
$X d^8 \sigma^2 \sigma^{*1} (^4\Phi)$		0 (0)	d	d	1300 ± 150 (930 ± 110)	1.67 ± 0.03 ^d (1.63 ± 0.03)

^aFor cases in which the state symmetry is not established, the most probable state assignment, is given in parentheses.

^bSpectroscopic constants for CoH were calculated using the isotope relations and the data for CoD reported in Ref. 22.

^cThe molecular constants for X (CoD) are taken from Ref. 22 for the X³Φ₄ state of CoD.

^dThe ω_e of the negative ions were set equal to the ν_{01} ($\omega_e x_e = 0$) for the Franck-Condon analyses, and hence the bond length reported for the negative ion corresponds to r_0 rather than r_e .

tion are ⁵Φ, ⁵Δ, and ⁵Π which are all accessible by one-electron allowed transitions from a CoH⁻ ⁴Φ($d^8 \sigma^2 \sigma^{*1}$). Qualitative arguments¹⁰ about the bonding of CoH predict the ⁵Φ state to be lowest in energy.

A Franck-Condon analysis has been performed on both of these transitions using the known spectroscopic constants²² for the ³Φ ground state of CoH to obtain ν_{01} and r_0 for the ground state of CoH⁻. These constants were then used in the analysis to obtain r_e for the final state of transition A. This analysis is similar to what has been previously published¹ for MnH and FeH. No attempt was made to determine constants for the fine structure components of these states. The electron affinity of CoH (CoD) is determined from the spectrum to be 0.671 ± 0.010 eV (0.680 ± 0.010 eV) and the excitation energy of the excited state of CoH (CoD) observed in transition A is found to be 6625 ± 110 cm⁻¹ (6756 ± 110 cm⁻¹). The spectroscopic constants determined from analysis of the spectra together with the known optical constants²² for the X³Φ ground state of CoH are summarized in Table I.

B. Spectra of NiH⁻ and NiD⁻

The photoelectron spectra of NiH⁻ and NiD⁻, taken with 2.54 eV photons, are shown in Fig. 3. Several peaks, labeled X, and A through D remain nearly unchanged in energy in the hydride and deuteride spectra, and are accordingly assigned as (0,0) transitions. A final state vibrational progression is built off of peak X with a separation between the (1,0) and (0,0) peaks of 1374 cm⁻¹ for the deuteride, in excellent agreement with optical data for ground X²Δ($d^9 \sigma^2$) state of NiD ($\nu_{01} = 1390.09$ cm⁻¹).²⁴ The (1,0) peak of the transition to the ground state of NiH overlaps with the (0,0) peak A, and an accurate determination of its energy is not possible.

The observation of a vibrational progression in the transition to the ground state is again in agreement with our qualitative model and the expectation that loss of a σ^* electron from a X³Δ($d^9 \sigma^2 \sigma^{*1}$) state of NiH⁻ results in a tran-

sition to the low-spin state of the neutral, with an accompanying large geometry change. There is further evidence for this assignment for the state of the negative ion. The ground ²Δ state of NiH is known²⁴ to have a spin-orbit splitting of 980 cm⁻¹. If the ground state of NiH⁻ were ¹Σ($d^{10} \sigma^2$), the only other plausible state, transitions to the two spin-orbit states of NiH would be resolved in the spectra. The lack of resolution of the two spin-orbit states is a strong indication

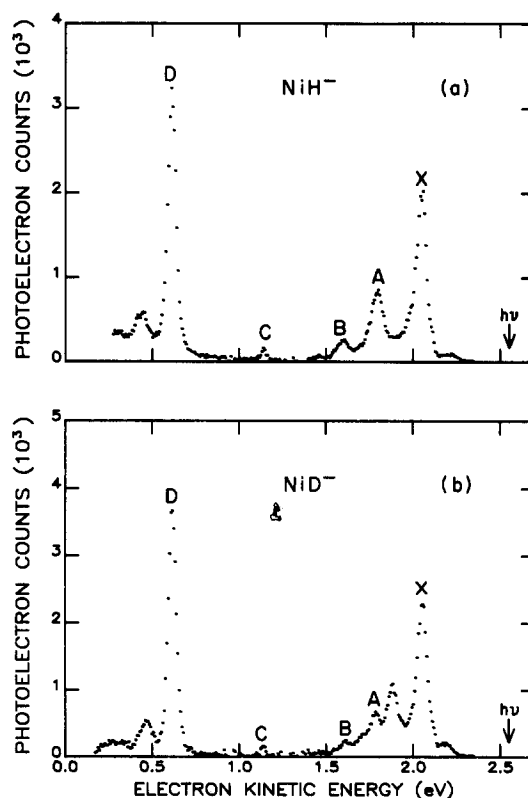


FIG. 3. Photoelectron spectra of NiH⁻ and NiD⁻ obtained with 488.0 nm (2.540 eV) photons. Peaks X and A through D correspond to (0,0) transitions in photodetachment.

for an orbitally degenerate ground state for the negative ion as well, causing a plethora of unresolved transitions between the two ground states.

Peak *D* shows a very weak final state vibrational progression in the spectra of both NiH⁻ and NiD⁻, with a vibrational frequency of $1650 \pm 210 \text{ cm}^{-1}$ for the hydride and $1190 \pm 150 \text{ cm}^{-1}$ for the deuteride. The intensity and nearly diagonal nature of this transition are similar to what has been previously observed in transitions to high-spin states for the other metal hydrides studied. We therefore assign this peak as due to a transition to a high-spin quartet state of $d^8 \sigma^2 \sigma^{*1}$ configuration. The lowered vibrational frequency for this state as compared to the ground state also supports this assignment. Both qualitative arguments¹⁰ and quantum mechanical calculations³² predict the $^4\Delta$ state to be the lowest in energy of the possible $^4\Phi$, $^4\Delta$, $^4\Pi$, and $^4\Sigma$ states with this configuration.

Peaks *A* and *B* are near an energy where strong perturbations have been observed²⁵ in the optical spectrum of NiH. These perturbations have been proposed²⁵ to result from interaction with a $^2\Pi$ state at about 2800 cm^{-1} above the vibrationless level of the ground state. Inordinately large lambda doubling suggests a nearby second perturber, probably a $^2\Sigma^+$ state. Several calculations have been reported on NiH³²⁻³⁸ with the most extensive treatment of the three lowest states being that of Blomberg *et al.*³² These authors predict the $^2\Pi$ ($d^9 \sigma^2$) state to be at 2431 cm^{-1} and the $^2\Sigma^+$ ($d^9 \sigma^2$) state to be at 2926 cm^{-1} excitation energy (T_e). Each of these two states would only be reached by a two-electron transition in photodetachment, but calculations indicate that states of the metal-hydrides are frequently highly mixed.¹⁰ We conclude that peaks *A* and *B* are due to transitions to the $^2\Pi$ and $^2\Sigma^+$ states. However, which state be-

longs to which peak cannot be unambiguously determined from the photoelectron spectra. Ongoing spectroscopic study of NiH by Field and co-workers²⁷ using the stimulated emission probe technique shows promise of providing assignments for all of the low-lying doublet states of NiH in the near future. The observation of peak *C* in both isotopic molecules leads us to identify it as belonging to the NiH molecule, but its identity is unknown.

The electron affinity of NiH (NiD) is determined from the spectra to be $0.481 \pm 0.007 \text{ eV}$ ($0.477 \pm 0.007 \text{ eV}$). Spectroscopic constants for NiH⁻ and the excited states of NiH observed in the spectra, as determined by peak fitting and Franck-Condon analysis, are summarized along with the known²⁴ optical constants for ground state NiH in Table II.

C. Spectra of CrH⁻ and CrD⁻

The photoelectron spectra of CrH⁻ and CrD⁻, recorded with 2.54 eV photons, are shown in Fig. 4. The peaks labeled *X'*, *X*, *A*, *B*, and *B'* in each of the spectra are relatively unchanged in position between the hydride and the deuteride, and are therefore assigned as (0,0) peaks. In order to assign these transitions further, we must examine the electronic structure of CrH. Gas-phase optical spectroscopy^{20,21} and ESR of the matrix-isolated molecule¹⁹ establish the ground state of CrH as $^6\Sigma^+$. The overwhelming stability of the $d^{k+1}s^2$ configuration³ of Cr⁻, and contributions from the hydride configuration $\text{Cr}(d^5s^1) + \text{H}^-(s^2)$, provide a firm basis for predicting a high-spin $^7\Sigma^+$ ($d^5\sigma^2\sigma^{*1}$) ground state for CrH⁻. One-electron photodetachment transitions between the CrH⁻ and CrH are thus expected to be as follows:

TABLE II. Spectroscopic constants for the states of NiH and NiH⁻ observed in the photoelectron spectra. The data for NiD and NiD⁻ are given in parentheses below the constants reported for the hydride species.

Predominant electron configuration and state assignment	EA (eV)	T_0 (cm ⁻¹)	ω_e (cm ⁻¹)	$\omega_e x_e$ (cm ⁻¹)	ν_{01} (cm ⁻¹)	r_f (Å)
NiH						
Peak <i>D</i> $d^8 \sigma^2 \sigma^{*1} (^4\Delta)^a$		11 610 ± 180 (11 620 ± 185)			1650 ± 210 ^b (1190 ± 150) ^b	1.52 ± 0.03 (1.53 ± 0.03)
Peak <i>C</i>		7 390 ± 130 (7 445 ± 170)
Peak <i>B</i> ($d^9 \sigma^2 ^2\Sigma^+$ or $^2\Pi$)		Not resolved (3 630 ± 100)				
Peak <i>A</i> ($d^9 \sigma^2 ^2\Pi$ or $^2\Sigma^+$)		Not resolved (2 230 ± 90)				
$X d^9 \sigma^2 ^2\Delta$	0.481 ± 0.007 (0.477 ± 0.007)	0 (0)	2003 ^c (1429) ^c	38.4 ^c (19.5) ^c	1926.6 ^c (1390.1) ^c	1.4756 ^d (1.4645) ^d
NiH ⁻						
$X d^9 \sigma^2 \sigma^{*1} (^3\Delta)$		0 (0)	e e	e e	1430 ± 200 ^e (1020 ± 140)	1.61 ± 0.03 (1.60 ± 0.03)

^a In the case for which the state symmetry or configuration is not known, the most probable assignment is given in parentheses.

^b Vibrational constants were determined from the vibrational frequency observed for NiD, and an assumed value for $\omega_e x_e^H = 30 \text{ cm}^{-1}$.

^c The ω_e and $\omega_e x_e$ for $^2\Delta_{5/2}$ of the neutral are derived from the isotope relations and the ν_{01} frequencies for the NiH and NiD from the optical data of Ref. 24, and used for the Franck-Condon analysis.

^d From the optical data, Ref. 24.

^e For the Franck-Condon analysis, $\omega_e x_e$ was set equal to zero, and ω_e assumed equal to the ν_{01} reported.

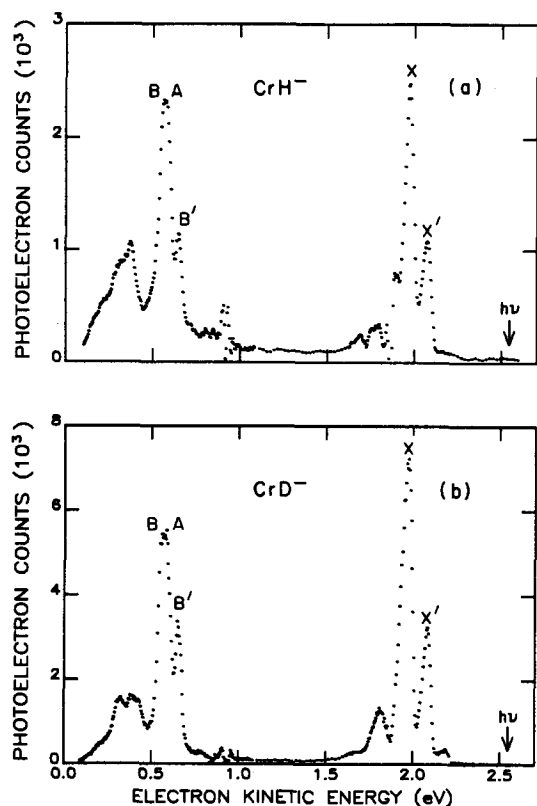
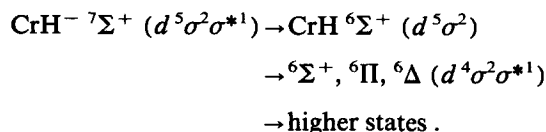


FIG. 4. Photoelectron spectra of CrH⁻ and CrD⁻ obtained with 488.0 nm (2.540 eV) photons. The peaks labeled X', X, A, B, and B' in each spectrum correspond to (0,0) transitions in the photodetachment. Scatter in the data points at about 0.9 eV and 1.8 eV electron kinetic energy is the result of statistical errors in the subtraction of the Cr⁻ contaminant spectrum.



The excited $^6\Sigma^+$ state is known from optical spectroscopy²¹ to have an excitation energy of $11\,552.29\text{ cm}^{-1}$. Additional excited states include the $^4\Sigma^+$, $^4\Pi$, and $^4\Delta$ states which arise from the low-spin coupling of the $d^4\sigma^2\sigma^*$ configuration, and other states resulting from different spin couplings of the d^5 core in the $d^5\sigma^2$ configuration of CrH. All of these states are expected to be much higher in energy than the excited sextet states and should be either absent or weak in the photoelectron spectrum as they would arise from two-electron transitions.

The observation of the two peaks, labeled X and X' in the spectra, only $810 \pm 80\text{ cm}^{-1}$ apart in CrH ($915 \pm 80\text{ cm}^{-1}$ in CrD) is quite surprising, since no low-lying excited states of CrH are expected. It therefore seems most plausible that the peak X' corresponds to a (0,0) transition from an electronically excited state of the negative ion. Changing source conditions often will change the populations of excited negative ion states, thus the relative intensity of the X and X' peaks. Although not dramatic, changes in the height of peak X' relative to X could be induced by varying the source conditions within the limited range of conditions under which the CrH⁻ ion could be produced, providing further cre-

dence for the anion excited state hypothesis.

Data analysis and assignment of the transitions in the spectra is rather limited, due to the existence of this excited electronic state of the negative ion. To further test the assignment of the (0,0) peak X as detachment to the ground state of the neutral, a vibrational frequency for the CrD is determined from the spectrum to be 1240 cm^{-1} , which compares to the gas-phase value^{20,21} of 1143 cm^{-1} (estimated from zero-point energy shifts). Although not in particularly good agreement, determination of the deuteride frequency from the photoelectron spectrum is complicated by overlap of Cr⁻ photodetachment (which has been subtracted out) and the presence of sequence bands. A Franck-Condon analysis yields a negative ion vibrational temperature of 1000 K, suggesting that the effect of sequence bands could be quite large. No attempt was made to determine the vibrational frequency in the hydride, due to the overlapping transitions and the difficulties in subtracting Cr⁻ transitions from this region of the spectrum.

For the excited state of CrD⁻, a well-resolved hot band was used to determine a vibrational frequency of $805 \pm 100\text{ cm}^{-1}$. Isotope relations give a vibrational frequency for the corresponding state of CrH⁻ (1125 cm^{-1}). A vibrational frequency for ground state CrH⁻ or CrD⁻ could not be determined from the spectrum, again due to overlapping peaks.

Analysis of the low electron kinetic energy portion of the spectrum is complicated by the presence of the excited CrH⁻ state. There are a few points worth noting. The peaks labeled A and B are a partially resolved doublet in both the hydride and deuteride spectra. Within this doublet, the X to B peak separation in the spectrum of CrH⁻ is $11\,500\text{ cm}^{-1}$, in good agreement with the $A\ ^6\Sigma^+$ excitation energy, $11\,552.29\text{ cm}^{-1}$, determined from optical data.²¹ This indicates the B peak arises from the $A\ ^6\Sigma^+$ (CrH) $\leftarrow X\ ^7\Sigma^+$ (CrH⁻) (0,0) transition. No assignment is possible for the A component of the doublet. The X' to B' peak separation is $11\,520\text{ cm}^{-1}$, again in good agreement with the $A\ ^6\Sigma^+$ excitation energy.

One likely possibility for the excited state of CrH⁻ is that it is an $a\ ^5\Sigma^+$ state, with a $d^5\sigma^2\sigma^*$ configuration in which the σ^* electron is low-spin coupled to the d^5 core. This assignment is strongly suggested by comparison to isoelectronic MnH,¹ which has an excited quintet state at 1720 cm^{-1} excitation energy. This assignment also predicts the one-electron transition $X\ ^6\Sigma^+ (d^5\sigma^2) \text{CrH} \leftarrow a\ ^5\Sigma^+ (d^5\sigma^2\sigma^*) \text{CrH}^-$, which would explain peak X'. A plausible assignment for the B' peak is thus the $A\ ^6\Sigma^+ (d^4\sigma^2\sigma^*) \text{CrH} \leftarrow a\ ^5\Sigma^+ (d^5\sigma^2\sigma^*) \text{CrH}^-$ transition.

Due to the difficulty in assigning the excited state of the negative ion, and the congestion at the low electron kinetic energy end of the spectrum, further assignment of the spectrum would be very speculative. Our observations provide an electron affinity of CrH (CrD) of $0.563 \pm 0.10\text{ eV}$ ($0.568 \pm 0.010\text{ eV}$). We observe an electronic excited state of the anion with excitation energy of $810 \pm 80\text{ cm}^{-1}$ in the hydride and $915 \pm 80\text{ cm}^{-1}$ in the deuteride. A Franck-Condon analysis gives a bond length of $1.75 \pm 0.05\text{ \AA}$ for both CrH⁻ states.

IV. DISCUSSION

The spectra reported here complete our study of the series of hydrides CrH through NiH , allowing us to probe periodic relationships in such parameters as excitation energies, vibrational frequencies, bond lengths, and electron affinities, which serve to test models of transition metal hydride electronic structure. We have modeled the spectra based upon a qualitative, single-configuration covalently bonded MH molecule, as discussed in the introduction and shown in Fig. 1. The photoelectron transitions from a high-spin MH^- state show distinctly different spectral signatures: a vibrational progression arises from the detachment to a low-spin MH state, while no progression should be observed following detachment to a high-spin MH state. The spectra of the Co and Ni hydrides reported here provide excellent corroboration of the spectral signatures seen in the MnH^- and FeH^- spectra. That is, they both show vibrational progressions in the transitions to the known low-spin ground states of the CoH and NiH molecules, with diagonal transitions to the excited high-spin states. The spectrum of CrH^- does not show quite the same distinctive signatures as those molecules. This might be expected, since the relative energies of the Cr atom states are such that the ground state with $d^5 s^1$ configuration is about 8000 cm^{-1} below the lowest $d^4 s^2$ based state.³⁹ This suggests somewhat different electronic configuration mixing in the molecular states than that illustrated in Fig. 1, which may be more appropriate for the metal atoms with $d^k s^2$ ground states.

One test of this single-configuration, covalent electronic structure model for the MH molecules is indicated by a plot of the energy difference in the high-spin and low-spin states, $T_0(d^{k+1} \sigma^2) - T_0(d^k \sigma^2 \sigma^{*1})$ (shown by the left vertical arrow in Fig. 1 connecting the molecular levels) as a function of the energy difference between the metal atom states from which they are derived, $E(d^{k+1} s^1) - E(d^k s^2)$ (shown by the right vertical arrow in Fig. 1). This correlation is shown in Fig. 5 for MnH , FeH , CoH , and NiH , those

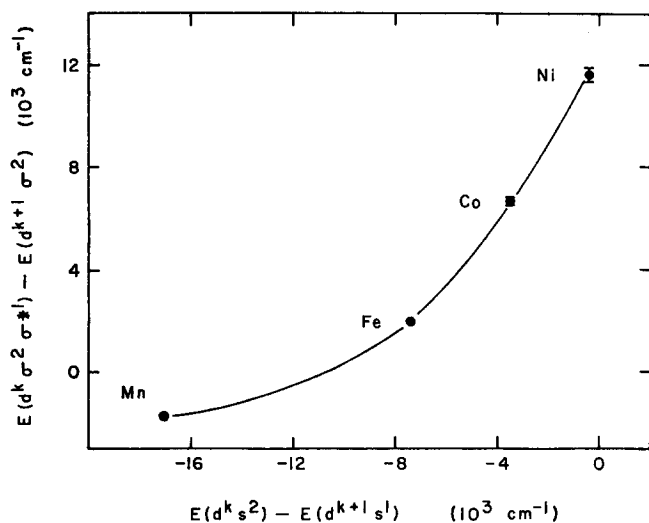


FIG. 5. Illustration of the correlation of the low-spin to high-spin energy separation in the MH molecules, $E(d^k \sigma^2 \sigma^{*1}) - E(d^{k+1} \sigma^2)$ with the atomic energy separation $E(d^k s^2) - E(d^{k+1} s^1)$. All data are taken from this work and Ref. 1.

molecules for which the atomic ground state has $d^k s^2$ configuration. A single-configuration molecular state would be expected to yield a linear relationship between these two energies. In fact, a nearly linear relationship is observed for the FeH , CoH , and NiH series, but the quintet state of MnH is considerably (8000 cm^{-1}) lower in energy than would be predicted from the single-configuration analysis. This departure from linearity for MnH suggests that configuration mixing, in particular, mixing of the $d^k \sigma^2 \sigma^{*1}$ configuration, in which the σ^{*1} electron is *low-spin* paired with the d^k core, with the $d^{k+1} s^2$ low-spin states should be particularly strong for the first excited quintet state⁴⁰ of MnH . This configuration mixing, although not as pronounced, is in large part responsible for the lowest quartet state of FeH having Δ symmetry.¹¹

One of the early puzzles facing several investigations in assigning the ground state configuration of FeH was the 1672 cm^{-1} gas phase vibrational frequency, obtained from the infrared spectrum of FeH at 4 K in an argon matrix. This frequency was considered anomalous in that it was intermediate between the 1490.2 cm^{-1} vibrational frequency observed for high-spin, $^7 \Sigma^+$ MnH , and the higher frequencies observed for the low-spin molecules, 1856 cm^{-1} for CoH and 1927 cm^{-1} for NiH . It therefore could not be used to readily identify FeH as having either a low- or high-spin configuration. In Fig. 6(a) the vibrational frequency for each of the low-spin states of the hydrides CrH through NiH is plotted as a function of increasing atomic number (that is, as the number of d electrons increases from 5 to 9). Indeed,

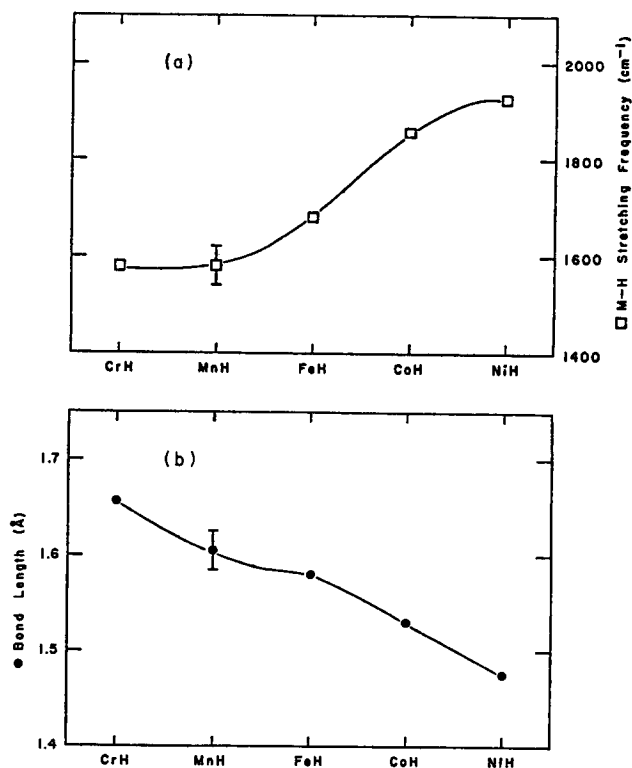


FIG. 6. Illustration of the changes in the 0 to 1 vibrational frequency (a) and bond length, r_e (b), for the low-spin states of the metal hydrides. In moving from CrH and NiH , the number of d electrons increases from 5 to 9 for the $d^k \sigma^2$ configuration of MH . All data except FeH (Refs. 8 and 9) are taken from this work or from Ref. 1.

there is no such *single* vibrational frequency for a low-spin hydride; rather, it increases with atomic number. Further indication of this may be found by plotting the bond length for the low-spin hydrides, CrH through NiH, as shown in Fig. 6(b). Again, a very regular change is observed, in this case a *decrease* in bond length with increasing atomic number, consistent with the *increase* in vibrational frequency. Shorter, stronger bonds with increasing vibrational frequencies are expected for the increasing nuclear charge and orbital contraction proceeding from CrH to NiH.

Similar trends are expected to hold for the vibrational frequencies and bond lengths for the high-spin states. Data on these states are extremely limited, however, since except for the ${}^7\Sigma^+$ ground state of MnH (and the possible inclusion of the ${}^6\Sigma^+$ state of CrH which has "high-spin" configuration $d^4\sigma^2\sigma^{*1}$), the *only* information on these states for FeH, CoH, and NiH is from the photoelectron spectra. The absence of vibrational progressions in the transitions to these states precludes the determination of accurate vibrational frequencies and bond lengths for these states from the present investigation.

Excluding CrH, there is a regular decrease in the EA for the low-spin states of MnH through NiH, as shown in Fig. 7(a), and there is seen to be a corresponding increase in the EA for the high-spin states, as shown in Fig. 7(b). The increase in EA for the high-spin states is exactly as expected for a core-electron loss, and mimics the increase in EA of the metal atoms⁴¹ with increasing nuclear charge. The EA for the low-spin states is the energy to remove the σ^* electron from the $d^{k+1}\sigma^2\sigma^{*1}$ MH⁻ ion. The observed decrease is

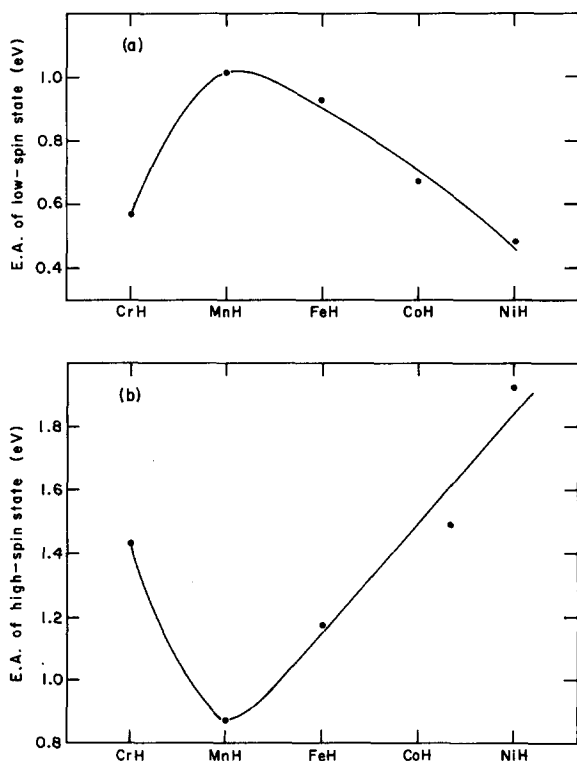


FIG. 7. Variation in the electron affinities for the low-spin states (a) and high-spin states (b) of the metal hydrides CrH through NiH. All data from this work and Ref. 1.

the opposite of the trend observed³¹ of increasing EA with atomic number for the transition metal atoms. A similar decrease with atomic number has been observed⁴² for the alkali halides, where decreasing EA appears to be correlated with the destabilization of the *s* electron of the alkali under the polarizing influence of the negatively charged halide as it comes in closer proximity to the alkali. For the metals here, this is mimicked by the decrease in the EA as an H⁻ approaches closer to the metal with configuration $d^{k+1}s^1$. For the alkali halides, the electron lost is the σ^* electron in the transition from a ${}^2\Sigma^+ MX^-$ to the ${}^1\Sigma^+ MX$ neutral. With the transition metals, the complex electronic structure suggests additional effects contribute to the trend of decreasing EA.

Finally, we note several periodic trends for the negative ions, with vibrational frequencies 1050 cm⁻¹ for MnH⁻, 1250 cm⁻¹ for FeH⁻,¹ 1300 cm⁻¹ for CoH⁻, and 1430 cm⁻¹ for NiH⁻, again showing a regular increase with atomic number. Similarly, the bond lengths decrease, from 1.82 Å for MnH⁻,¹ 1.74 Å for FeH⁻,⁴³ 1.67 Å for CoH⁻, and 1.61 Å for NiH⁻. Again CrH⁻, with a bond length of 1.75 Å, does not fit this trend, and suggests qualitatively different electronic structure.

ACKNOWLEDGMENTS

Support of this work by the National Science Foundation Grant Nos. PHY86-04504 and CHE83-16628 is gratefully acknowledged. Professor R. W. Field provided many stimulating discussions and insight on the configuration mixing in the metal hydrides and their negative ions. We also thank S. M. Burnett and K. K. Murray for their work in changing many of the data-handling programs for use with data from the new analyzer.

¹A. E. Stevens, C. S. Feigerle, and W. C. Lineberger, *J. Chem. Phys.* **78**, 5420 (1983).

²Calculations indicate that for the early transition metals, such as Sc and Ti, the hydrogen may bond to the *d* electron; see C. W. Bauschlicher, Jr. and S. P. Walch, *J. Chem. Phys.* **76**, 4560 (1982), and Ref. 15.

³C. S. Feigerle, R. R. Corderman, S. V. Bobashev, and W. C. Lineberger, *J. Chem. Phys.* **74**, 1580 (1981).

⁴T. E. Nevin and D. V. Stephens, *Proc. R. Ir. Acad.* **55**, 109 (1953).

⁵W. Hayes, P. D. McCarvill, and T. E. Nevin, *Proc. Phys. Soc. London Sect. A* **70**, 904 (1957).

⁶I. Kovács and P. Pacher, *J. Phys. B* **8**, 796 (1975).

⁷R. J. Van Zee, T. C. DeVore, J. L. Wilkerson, and W. Weltner, Jr., *J. Chem. Phys.* **69**, 1869 (1978).

⁸W. J. Balfour, B. Lindgren, and S. O'Connor, *Chem. Phys. Lett.* **96**, 251 (1983).

⁹W. J. Balfour, B. Lindgren, and S. O'Connor, *Phys. Scr.* **28**, 551 (1983).

¹⁰S. P. Walch and C. W. Bauschlicher, Jr., *J. Chem. Phys.* **78**, 4597 (1983).

¹¹S. P. Walch, *Chem. Phys. Lett.* **105**, 54 (1984).

¹²M. Krauss and W. J. Stevens, *J. Chem. Phys.* **82**, 5584 (1985).

¹³D. P. Chong, S. P. Walch, and H. Partridge, *J. Chem. Phys.* **85**, 2850 (1986).

¹⁴M. Dolg, U. Wedig, H. Stoll, and H. Preuss, *J. Chem. Phys.* **86**, 2123 (1987).

¹⁵R. R. Squires, *J. Am. Chem. Soc.* **107**, 4385 (1985).

¹⁶L. Sallans, K. R. Lane, R. R. Squires, and B. S. Freiser, *J. Am. Chem. Soc.* **107**, 4379 (1985).

¹⁷R. J. Van Zee, D. A. Garland, and W. Weltner, Jr., *J. Chem. Phys.* **84**, 5968 (1986).

- ¹⁸T. D. Varberg, J. A. Gray, and R. W. Field, Abstract PHYS 115, Abstracts of the 193rd ACS National Meeting, Denver, CO, April 1987.
- ¹⁹R. J. Van Zee, T. C. DeVore, and W. Weltner, Jr., *J. Chem. Phys.* **71**, 2051 (1979).
- ²⁰B. Kleman and U. Uhler, *Can. J. Phys.* **37**, 537 (1959).
- ²¹S. O'Connor, *Proc. R. Ir. Acad. Sect. A* **65**, 95 (1967).
- ²²L. Klynning and M. Kronekvist, *Phys. Scr.* **6**, 61 (1972); **7**, 72 (1973).
- ²³R. E. Smith, *Proc. R. Soc. London Ser. A* **332**, 113 (1973).
- ²⁴N. Åslund, H. Neuhaus, A. Lagerqvist, and E. Andersén, *Ark. Fys.* **28**, 271 (1964).
- ²⁵R. Scullman, S. Löfgren, and S. A. Kadavathu, *Phys. Scr.* **25**, 295 (1982).
- ²⁶J. A. Gray, S. F. Rice, and R. W. Field, *J. Chem. Phys.* **82**, 4717 (1985).
- ²⁷J. A. Gray and R. W. Field, Abstract PHYS 116, Abstracts of the 193rd ACS National Meeting, Denver, CO, April 1987.
- ²⁸R. J. Celotta, R. A. Bennett, and J. L. Hall, *J. Chem. Phys.* **60**, 1740 (1974); M. W. Siegel, R. J. Celotta, J. L. Hall, J. Levine, and R. A. Bennett, *Phys. Rev. A* **6**, 607 (1972).
- ²⁹C. S. Feigerle, Ph.D. thesis, University of Colorado, 1983; D. G. Leopold, K. K. Murray, A. E. S. Miller, and W. C. Lineberger, *J. Chem. Phys.* **83**, 4849 (1985).
- ³⁰R. R. Corderman, P. C. Engelking, and W. C. Lineberger, *J. Chem. Phys.* **70**, 4474 (1979).
- ³¹A. E. S. Miller, C. S. Feigerle, and W. C. Lineberger, *J. Chem. Phys.* **84**, 4127 (1986).
- ³²M. R. A. Blomberg, P. E. M. Siegbahn, and B. O. Roos, *Mol. Phys.* **47**, 127 (1982).
- ³³M. P. Guse, R. J. Blint, and A. B. Kunz, *Int. J. Quantum Chem.* **11**, 725 (1977).
- ³⁴B. I. Dunlap and H. L. Yu, *Chem. Phys. Lett.* **73**, 525 (1980).
- ³⁵P. S. Bagus and C. Bjorkman, *Phys. Rev. A* **23**, 461 (1981).
- ³⁶S. P. Walch and C. W. Bauschlicher, Jr., *Chem. Phys. Lett.* **86**, 66 (1982).
- ³⁷L. G. M. Pettersson, U. Wahlgren, and O. Gropen, *Chem. Phys.* **80**, 7 (1983).
- ³⁸F. Ruetter, G. Blyholder, and J. Head, *J. Chem. Phys.* **80**, 2042 (1984).
- ³⁹C. E. Moore, *Natl. Bur. Stand. (U.S.) Circ.* 467 (U. S. GPO, Washington, D. C., 1958).
- ⁴⁰The existence of a low-lying quintet state of MnH was confirmed in Ref. 1. We suggested at that time that, of the possible $^5\Delta$, $^5\Pi$, and $^5\Sigma$ states of $d^6\sigma^2$ configuration, the most probable assignment for this state was $^5\Delta$. However, only the $^5\Sigma(d^6\sigma^2)$ can mix with the $^5\Sigma(d^5\sigma^2\sigma^{*1})$, the one state which can be formed from low-spin coupling of σ^* to the high-spin d^5 core. The data in Fig. 5 suggest this interaction to be particularly strong and argue for a $^5\Sigma$ assignment for the lowest MnH quintet state observed in the photodetachment spectrum of MnH^- and consequently a $^6\Sigma$ assignment for MnH^- . A definitive assignment for this MnH quintet state awaits a rigorous optical spectroscopic analysis.
- ⁴¹H. Hotop and W. C. Lineberger, *J. Phys. Chem. Ref. Data* **14**, 731 (1985).
- ⁴²T. M. Miller, D. G. Leopold, K. K. Murray, and W. C. Lineberger, *J. Chem. Phys.* **85**, 2368 (1986).
- ⁴³The bond length for FeH^- is determined from Franck-Condon analysis of Ref. 1, but using a more recent determination for the bond length of FeH , $r_e = 1.58 \text{ \AA}$ (Refs. 8 and 9).